Electronic Supplementary Material (ESI) for RSC Advances.
This journal is © The Royal Society of Chemistry 2021

Fabrication of TiO_2-supported clinoptilolite via F^- contained hydrothermal etching and resultant highly energetic {001} facet for enhancement of its photocatalytic activity

Raza Ullah, Jihong Sun*, Anadil Gul, Tallat Munir, Shiyang Bai*

Beijing Key Laboratory for Green Catalysis and Separation, Department of Environmental and Chemical Engineering, Beijing University of Technology, Beijing 100124, P. R. China

Electronic Supporting Information

Captions of Figures and Tables

Fig. S1. Schematic illustration of the synthesis of TiO_2/CPs.

Fig. S2. XRD patterns (A) of (a) ACP2, (b) ACP5, and (c) ACP7 and FT-IR spectra (B) of (a) ACP1, (b) ACP2, (c) ACP4, (d) ACP5, (e) ACP7, and (f) anatase TiO_2.

Fig. S3. SEM images of (a) ACP2, (b) ACP5, and (c) ACP7.

Fig. S4. Pore size distribution curves of TiO_2/CPs deriving from the desorption branch of the isotherms on the BJH model.

Fig. S5. Effect of various catalysts on the photo-catalytic degradation of CV (A) and MO (B) dyes. (a) ACP2, (b) ACP5, and (c) ACP7. Conditions: Initial concentration of dye = 0.0245 mM, catalyst dose = 0.5g/L, pH = 6.0, Room temperature.

Fig. S6. Effect of UV-light alone (a and c), and bare CP (b and d) on the degradation of CV (a and b) and MO (c and d) dyes, respectively.

Fig. S7. A: Effect of irradiation time on the photo-catalytic degradation of CV (a) and MO (b) dyes. B: UV-Vis absorbance spectra of CV. C: UV-Vis absorbance spectra of MO at different irradiation time intervals, catalyzed by ACP6. Conditions: Initial concentration of dye = 0.0245 mM, catalyst dose = 0.75 g/L, pH = 8.0, Time = 120 min, and Room temperature.

Fig. S8. Effect of radicals scavengers on the photocatalytic degradation of CV and MO dyes, a: CV degradation without scavengers, b: MO degradation without scavengers, c: CV degradation in the presence of isopropyl alcohol, d: MO degradation in the

presence of isopropyl alcohol, e: CV degradation in the presence of benzoquinine, and f: MO degradation in the presence of benzoquinine.

Fig. S9. Proposed degradation mechanisms of (a) CV and (b) MO dyes.

Table S1. Crystallinity of loaded TiO_2 and CP supports and ratio of the high energy {004} and low energy {101} facet.

Table S2. Pseudo-first order rate constant of CV and MO dyes using different kinds of catalysts.

Table S3. Observed rate constants and degradation (%) of CV and MO dyes using ACP6 as photocatalyst at different initial concentration of the dyes.

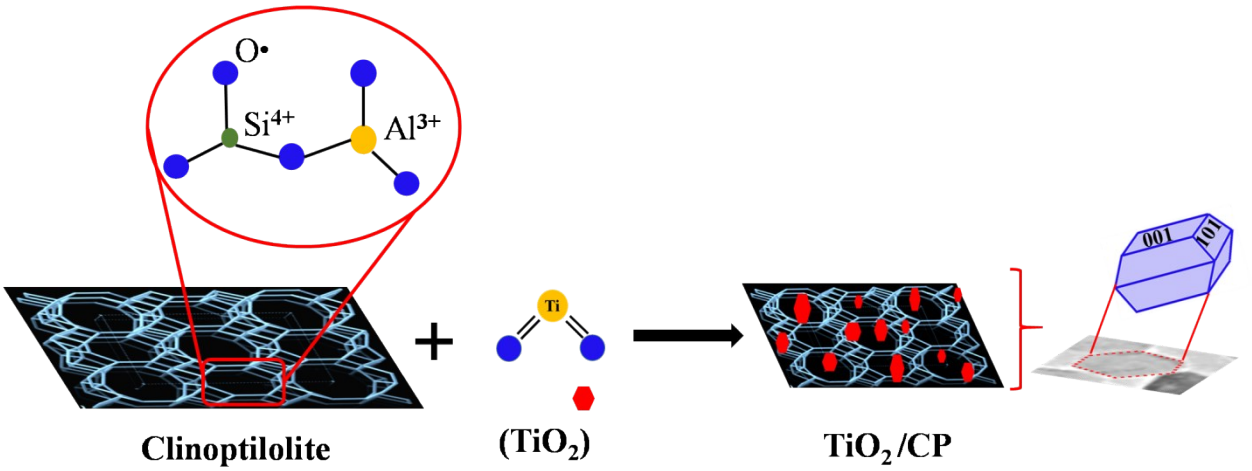

Fig. S1. Schematic illustration of the synthesis of TiO_2/CPs.

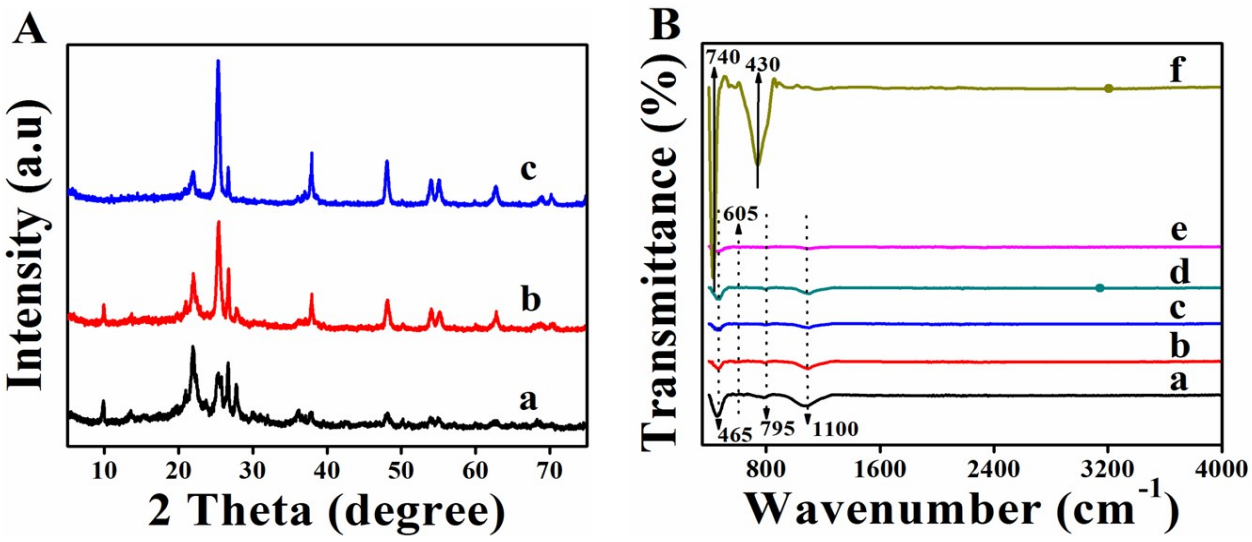

Fig. S2. XRD patterns (A) of (a) ACP2, (b) ACP5, and (c) ACP7 and FT-IR spectra (B) of (a) ACP1, (b) ACP2, (c) ACP4, (d) ACP5, (e) ACP7, and (f) anatase TiO_2.

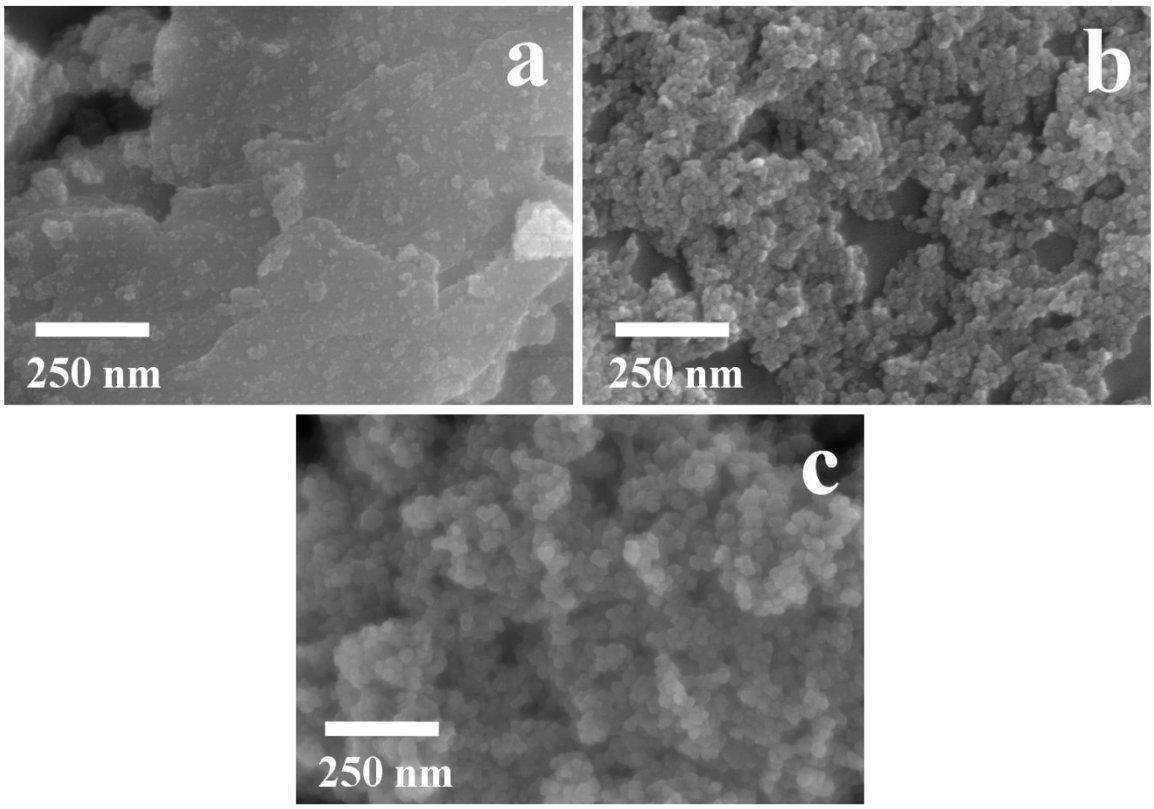

Fig. S3. SEM images of (a) ACP2, (b) ACP5, and (c) ACP7.

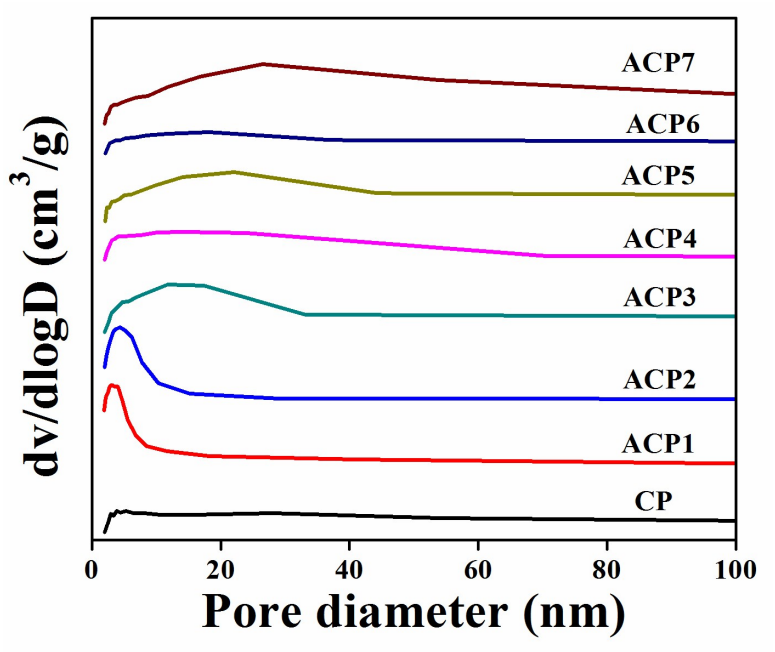

Fig. S4. Pore size distribution curves of TiO_2/CPs deriving from the desorption branch of the isotherms on the BJH model.

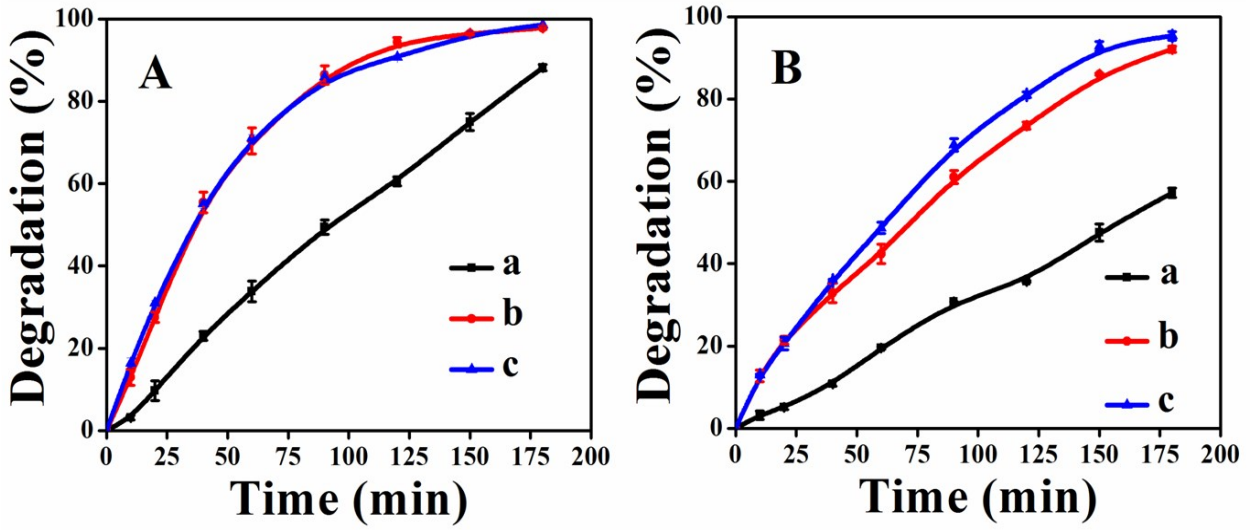

Fig. S5. Effect of various catalysts on the photo-catalytic degradation of CV (A) and MO (B) dyes. (a) ACP2, (b) ACP5, and (c) ACP7. Conditions: Initial concentration of dye = 0.0245 mM, catalyst dose = 0.5g/L, pH = 6.0, Room temperature.

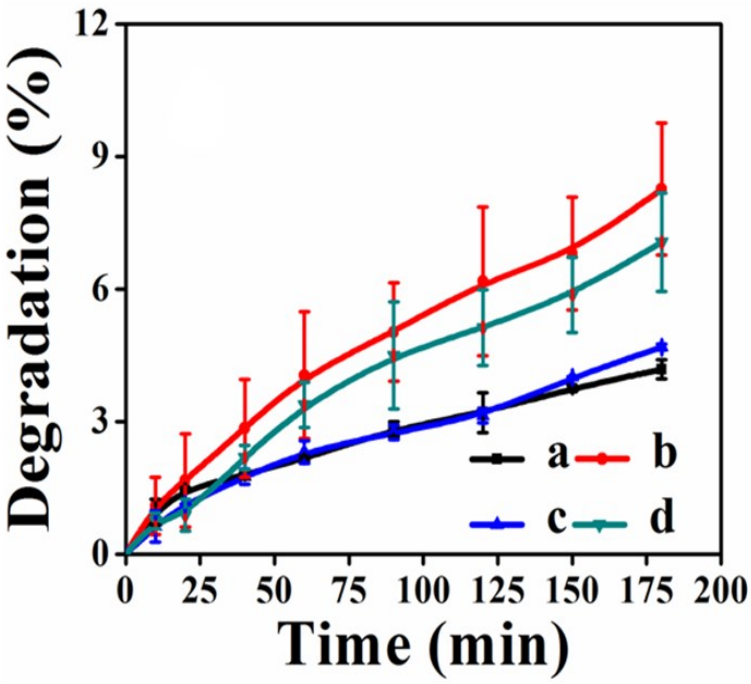

Fig. S6. Effect of UV-light alone (a and c), and bare CP (b and d) on the degradation of CV (a and b) and MO (c and d) dyes, respectively.

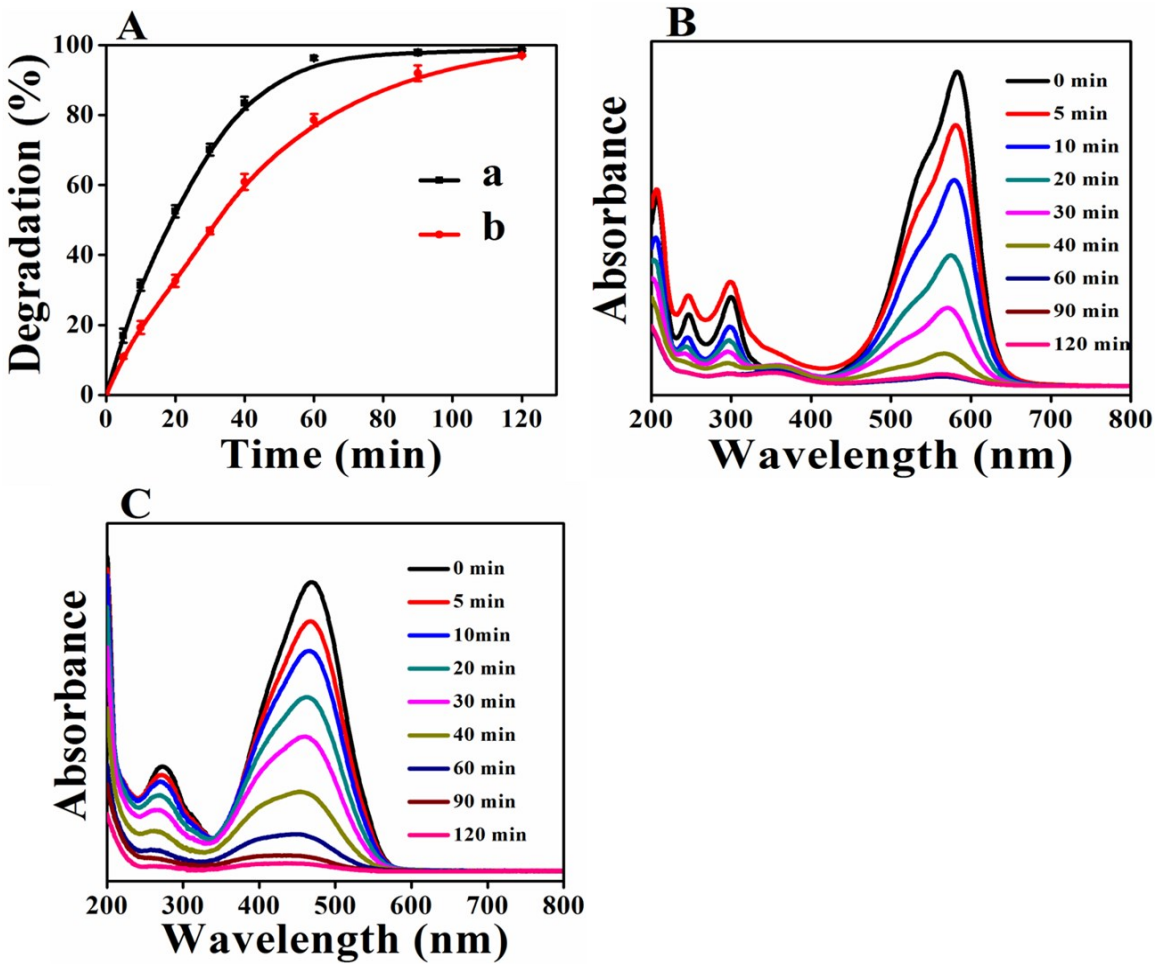

Fig. S7. A: Effect of irradiation time on the photo-catalytic degradation of CV (a) and MO (b) dyes. B: UV-Vis absorbance spectra of CV. C: UV-Vis absorbance spectra of MO at different irradiation time intervals, catalyzed by ACP6. Conditions: Initial concentration of dye = 0.0245 mM, catalyst dose = 0.75 g/L, pH = 8.0, Time = 120 min, and Room temperature.

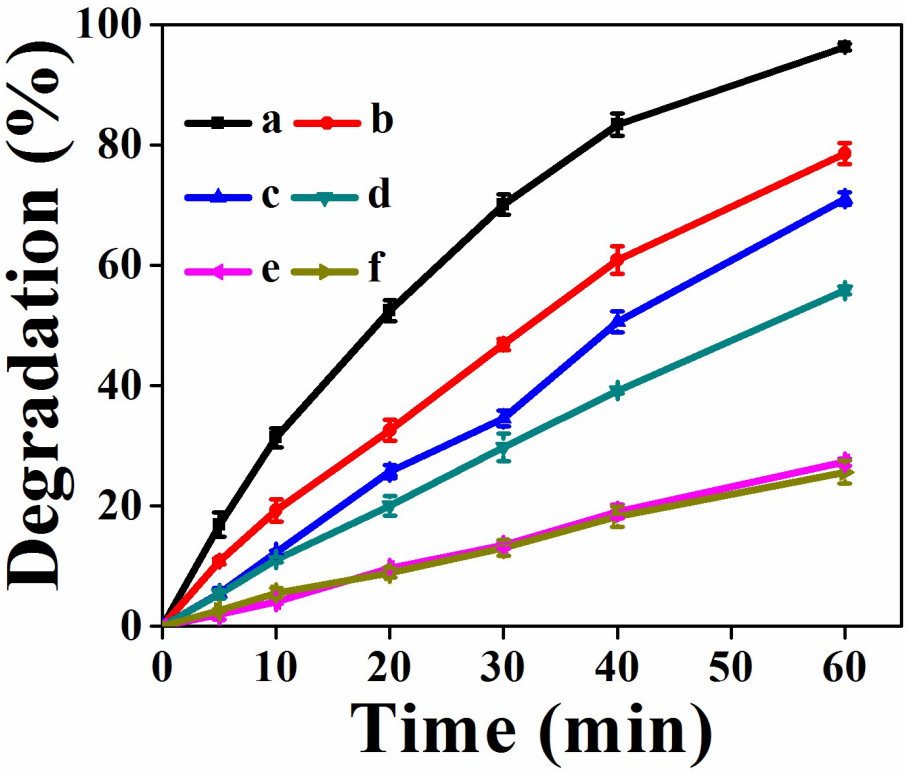

Fig. S8. Effect of radicals scavengers on the photocatalytic degradation of CV and MO dyes, a: CV degradation without scavengers, b: MO degradation without scavengers, c: CV degradation in the presence of isopropyl alcohol, d: MO degradation in the presence of isopropyl alcohol, e: CV degradation in the presence of benzoquinine, and f: MO degradation in the presence of benzoquinine.

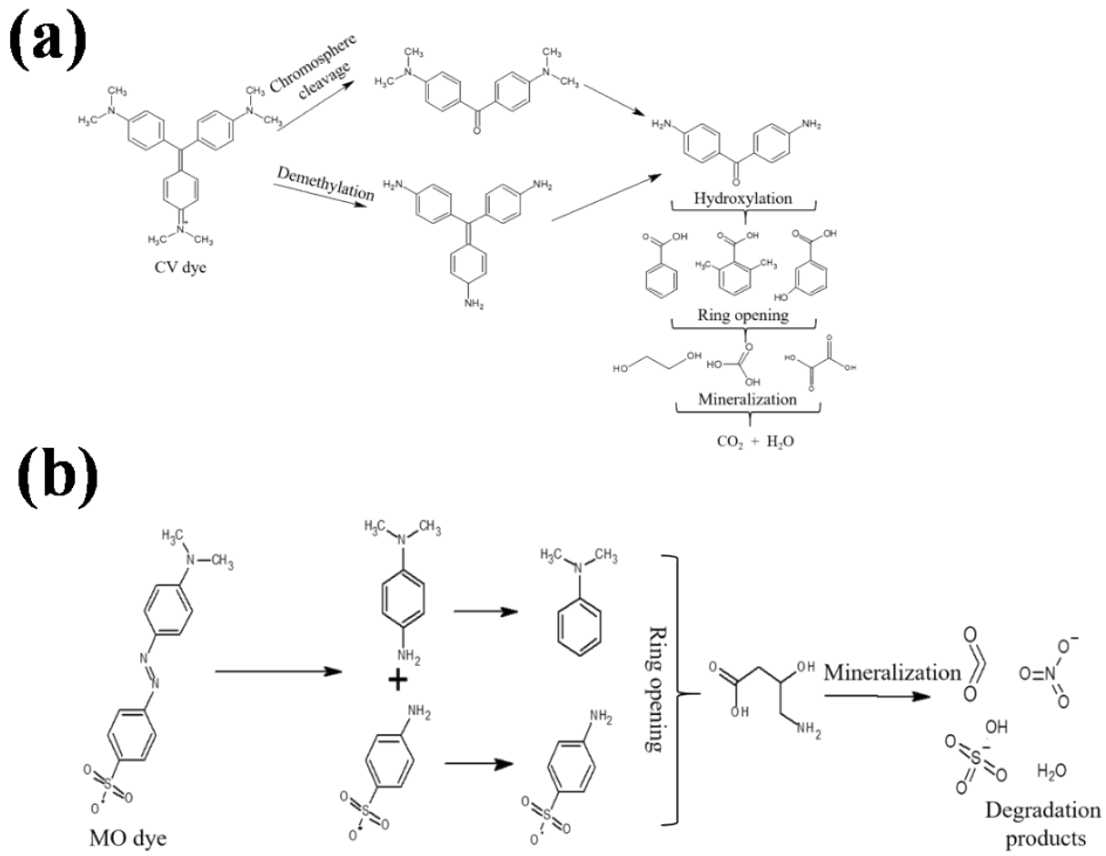

Fig. S9. Proposed degradation mechanisms of (a) CV and (b) MO dyes.

Table S1. Crystallinity of loaded TiO_2 and CP supports and ratio of the high energy {004} and low energy {101} facet.

Sample	Crystallinity (%) of loaded TiO_2 inTiO_2/CP	I_{004}/I_{101}	Crystallinity (%) of CP
CP	-	-	100
ACP1	37.90	0.26	48.10
ACP2	42.13	0.24	61.39
ACP3	52.04	0.28	58.62
ACP4	54.33	0.32	46.31
ACP5	68.36	0.36	46.31
ACP6	77.53	0.38	45.33
ACP7	83.74	0.38	27.08
TiO_2	100	0.30	-

Table S2. Pseudo-first order rate constant of CV and MO dyes using different kinds of catalysts.

Catalyst type	CV		MO	
	k_{app} (min^{-1})	R^2	k_{app} (min^{-1})	R^2
ACP1	0.007	0.996	0.004	0.999
ACP2	0.007	0.990	0.003	0.975
ACP3	0.008	0.985	0.004	0.989
ACP4	0.016	0.996	0.008	0.994
ACP5	0.021	0.994	0.008	0.986
ACP6	0.022	0.998	0.012	0.999
ACP7	0.020	0.998	0.010	0.995
TiO_2	0.015	0.994	0.008	0.995

Table S3. Observed rate constants and degradation (%) of CV and MO dyes using ACP6 as photocatalyst at different initial concentration of the dyes.

Dye	Dye concentration (mM)	Degradation (%)	k_{app} (min^{-1})	R^2
CV	0.0122	94	0.069	0.993
	0.0245	77	0.037	0.988
	0.0368	62	0.024	0.992
	0.0490	51	0.017	0.987
MO	0.0122	76	0.035	0.991
	0.0245	61	0.026	0.984
	0.0368	43	0.014	0.984
	0.0490	31	0.010	0.977